CRISPR-TSKO facilitates efficient cell type-, tissue-, or organ-specific mutagenesis in Arabidopsis

Ward Decaestecker[1,2,#], Rafael Andrade Buono[1,2,#], Marie L. Pfeiffer[1,2], Nick Vangheluwe[1,2], Joris Jourquin[1,2], Mansour Karimi[1,2], Gert Van Isterdael[3,4], Tom Beeckman[1,2], Moritz K. Nowack[1,2,*], and Thomas B. Jacobs[1,2,*]

1. Ghent University, Department of Plant Biotechnology and Bioinformatics, Technologiepark 927, 9052 Ghent, Belgium
2. VIB Center for Plant Systems Biology, Technologiepark 927, 9052 Ghent, Belgium
3. VIB Flow Core, VIB Center for Inflammation Research, Technologiepark 927, B-9052 Ghent, Belgium.
4. Department of Internal Medicine, Ghent University, Ghent, Belgium.

[#] These authors contributed equally to the manuscript
*Corresponding authors: TBJ thjac@psb.vib-ugent.be, MKN moritz.nowack@vib.be

Abstract

Detailed functional analyses of many fundamentally important genes via conventional loss-of-function approaches are impeded by severe pleiotropic phenotypes. In particular, mutations in genes that are required for basic cellular functions or plant reproduction often interfere with the generation of homozygous mutant plants precluding further functional studies. To overcome this limitation, we devised a CRISPR-based tissue-specific knockout system, CRISPR-TSKO, enabling us to generate mutations in particular plant cell types, tissues, and organs. In Arabidopsis, resulting somatic mutations even in essential genes caused well-defined, localized phenotypes with high efficiency in the root cap, stomatal lineage, or in entire lateral roots. The underlying modular cloning system allows for efficient selection, identification, and functional analysis of mutant lines directly in the first transgenic generation. The efficacy of CRISPR-TSKO opens new avenues to analyze gene functions in virtually any given spatial and temporal context of plant life while avoiding pleiotropic effects of system-wide loss of gene function.

Introduction

The generation of stable, inheritable loss-of-function mutant alleles has been indispensable for functional genomics studies in plants. Such knockout or knockdown lines have been generated with various techniques such as ionizing radiation, ethyl methanesulfonate, T-DNA or transposon insertions, RNA interference (RNAi), or artificial microRNAs. In recent years there has been an explosion in the generation of plant lines mutated by clustered regularly interspaced short palindromic repeat (CRISPR) gene knockout.

CRISPR technology contains two components, the CRISPR-associated (Cas) nuclease and CRISPR RNAs (crRNA) that direct the nuclease to the target nucleic acid. The most widely used CRISPR system in plants is based on the DNA endonuclease Cas9 and its artificial crRNA, the guide RNA (gRNA)[1]. In plants, Cas9 is very efficient at inducing double-stranded breaks in DNA. The DNA breaks repaired by the error-prone non-homologous end joining pathway ultimately result in the formation of short insertions and/or deletions (indels) at the break site[2]. These indels most often lead to frame shifts and early stop codons, facilitating an effective knock-out of the targeted gene(s).

Most, if not all, CRISPR efforts to date have focused on generating stable and inheritable DNA mutations in plants for reverse genetics approaches. Yet the ability to study essential genes is limited using this approach as loss of many fundamentally-important genes convey severe pleiotropic phenotypes up to lethality. Of the approximately 25,000 protein-coding genes in the *Arabidopsis thaliana* genome, 10% are estimated to be indispensable[3], presenting a considerable challenge for functional analyses especially of genes with essential functions.

An approach to overcome these problems is the use of tissue-specific RNAi[4]. However, gene silencing is often incomplete, interfering with the interpretation of the observed phenotypes. Furthermore, small RNAs can be mobile, limiting tissue specificity[5]. Therefore, the results obtained using RNAi are often not comparable with the use of stably transmitted DNA-based mutants. For certain genes, transgenic vectors generating dominant-negative protein versions have been developed. Expressing these mutant versions in a tissue-specific context can locally interfere with endogenous gene

functions[6, 7]. Other methods include the conditional knockout of genes in specific cell types or tissues by using a CRE-recombinase[8]. These approaches, however, can be cumbersome and difficult to scale up[9].

Outside of the plant field, researchers have recently overcome such limitations with the development of conditional knockouts using CRISPR technology. In zebrafish, the *gata1* promoter driving Cas9 expression has been used to knockout genes specifically in the erythrocytic lineage[10]. In Drosophila, targeted knockout mutations in two essential genes *Wingless* and *Wntless* only in germ cells permitted the generation of adult flies, whereas constitutive knockout individuals did not survive past the pupal stage[11]. Additionally, cardiomyocyte-specific expression of Cas9 led to organ-specific knockout in a mouse model[12]. In plant research, however, analogous approaches have not been reported thus far.

Here, we describe the development of a CRISPR **t**issue-**s**pecific **k**nock-**o**ut (CRISPR-TSKO) system in Arabidopsis that allows for the specific generation of somatic DNA mutations in plants. The CRISPR-TSKO toolset is simple to use, highly efficient and allows for multiplexing and large-scale screening approaches. We show the potential CRISPR-TSKO for somatic gene knockouts of essential genes in diverse plant cell types, tissues, and even entire organs. Our approach opens new opportunities to study the function of fundamentally important genes in specific contexts of plant biology.

Results

Tissue specific GFP knockout in the lateral root cap

We reasoned that by utilizing tissue-specific promoters to drive Cas9 expression, CRISPR could be used to generate cell type-, tissue-, and organ-specific DNA mutations with high precision. To test this hypothesis, T-DNA vectors were constructed with Cas9 expression controlled by the promoter region of *SOMBRERO*/*ANAC033* (*SMB*; AT1G79580). The *SMB* promoter (*pSMB*) is highly root cap-specific and is activated directly after the formative division of root cap stem cells[13, 14]. The *pSMB*:Cas9 expression cassette was combined with one of two individual U6-expressing gRNAs targeting the GFP coding sequence, GFP-1 and GFP-2, and transformed into a homozygous Arabidopsis line with ubiquitous expression of a nuclear-localized GFP and

β-glucuronidase (GUS) fusion protein (pHTR5:NLS-GUS-GFP[15], henceforth, NLS-GFP). Primary transgenic plants (T1 seedlings) were selected via resistance to the herbicide glufosinate and investigated for loss of GFP signal in the root tips of five-day-old seedlings. Strikingly, six out of eleven *pSMB*:Cas9;GFP-1 events and three out of ten *pSMB*:Cas9;GFP-2 events showed an almost complete loss of GFP specifically in the root cap, suggesting high efficiency CRISPR-mediated knockout soon after the formative division of the root cap stem cells (**Supplementary Fig. 1a**). All other root tissues maintained GFP expression, indicating that specific Cas9 activity in the root cap cells led to cell-autonomous GFP knockout. The tissue-specific effect is heritable, as three lines with *pSMB*:Cas9;GFP-1 and three lines with *pSMB*:Cas9;GFP-2, had T2 progeny without GFP fluorescence in root cap cells while having normal NLS-GFP expression in all other tissues examined (**Supplementary Fig. 1b**). These results clearly indicated that the use of a tissue-specific promoter driving Cas9 can result in somatic, tissue-specific knockout phenotypes.

Design of the CRISPR-TSKO gene knockout toolset

While we were encouraged by these initial results, two limitations were identified: (1) the specific expression of Cas9 in each line could not be easily monitored; and (2) herbicide selection on the T1 seedlings caused stress and limited the ability to directly phenotype primary transgenic T1 seedlings. To overcome these limitations, and to facilitate a wide range of future gene-modification approaches, we devised CRISPR-TSKO, a modular and versatile vector toolset based on Golden Gate technology using modified GreenGate vectors[16, 17]. CRISPR-TSKO is thus inexpensive and immediately compatible with modules already in use by other laboratories that have adopted the GreenGate vector system. The modularity allows for the combination of Cas9, or any nuclease, with virtually any promoter sequence of choice. Furthermore, Cas9 protein fusions are possible on the N- and C-termini allowing for the wide range of CRISPR technologies such as base editors[18] or transcriptional regulators[19]. The promoter, Cas9, N- and C-tags, and terminator modules can be combined with an “unarmed” gRNA cassette to generate an unarmed destination vector (**Fig. 1**). One or two gRNAs can be directly cloned into the destination vector with a single Golden Gate reaction (see methods).

Alternatively, when an AarI linker is used instead of the unarmed gRNA cassette, a second round of Golden Gate assembly can be performed for the cloning of up to 12 gRNAs in a single destination vector (**Supplementary Fig. 2**).

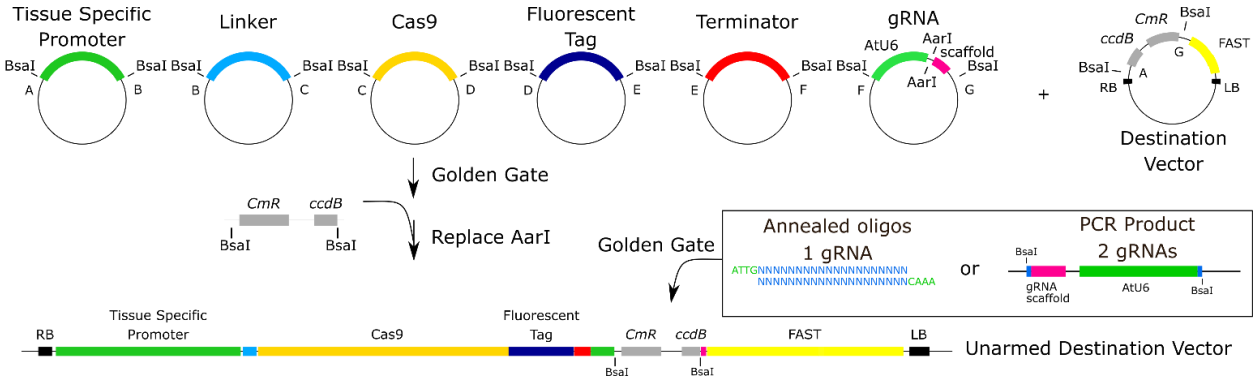

Fig. 1: Cloning workflow for CRISPR vectors

Six entry modules are combined in a binary destination vector, containing a FAST screenable marker cassette, with Golden Gate assembly. The six entry modules contain a tissue specific promoter, a cloning linker, the Cas9 nuclease, a fluorescent tag, a terminator and a module containing an AtU6-26 promoter driving the expression of an unarmed gRNA scaffold. These modules replace the *ccd*B and *Cm*R selectable markers allowing for the negative selection of the destination vector in *ccd*-sensitive *E. coli* cells. The resulting vector can be directly 'armed' with one or two gRNA's, upon pre-digestion with AarI. Alternatively, these AarI restriction sites can be replaced by a PCR product containing two BsaI sites flanking a ccdB and CmR. The resulting vector can be 'armed' via a Golden Gate reaction without the AarI pre-digestion and allows for the negative selection in *ccd*-sensitive *E. coli* cells. In a single Golden Gate reaction, a pair of annealed oligo's can be cloned, resulting in an expression vector containing one gRNA. Alternatively, Golden Gate cloning of a PCR product containing a first gRNA attached to an AtU6-26 promoter and the protospacer sequence of the second gRNA, results in an expression vector containing to gRNAs.

A collection of binary destination vectors that contain different selectable markers and/or a non-destructive fluorescent markers based on the fluorescence-accumulating seed technology (FAST) system[20] were generated to take advantage of this general cloning strategy (**Supplementary Table 3**). The FAST system allows for the antibiotic- or herbicide-free selection of transformed T1 seeds, and permits a time-saving screening for phenotypes directly in T1 seedlings. To facilitate the determination of tissue specificity and expression levels of Cas9, a nuclear-localized fluorescent mCherry tag to was fused to the Cas9 transcript via a P2A ribosomal skipping peptide[21]. Using this strategy we targeted different tissue types, cell lineages, and organs in Arabidopsis to explore the potential of CRISPR-TSKO in plants.

Root-cap specific gene knockout

Utilizing CRISPR-TSKO, Cas9-mCherry was expressed under *pSMB* and combined with the gRNA GFP-1. Ten of the 21 T1 seedlings showed a complete loss of GFP fluorescence specifically in the root cap, while six showed partial loss of GFP (chimeras), and five maintained normal GFP expression (**Fig. 2a, Table 1**). Of note, even in strong knock-out lines, cells of the youngest root cap layers retained some GFP signal (**Fig. 2b**). This result suggests that mRNA and/or protein turnover is required after the onset of Cas9 expression for the phenotype to become apparent. Interestingly, we could observe a clear correlation between the intensity of mCherry expression and the penetrance of the knockout phenotype. All ten highly-expressing mCherry lines were entirely devoid of root-cap GFP signal, the medium mCherry-expressing lines had chimeric knockout phenotype and the low-to-no mCherry lines had chimeric or full expression of GFP (**Table 1**). By comparing the intensity of both fluorescent proteins in root cap nuclei, we confirmed our observations that higher Cas9 expressing lines have a significantly higher probability of gene editing success (**Fig. 2c**).

Table 1. Phenotypes of T1 seedlings transformed with *pSMB*:Cas9-mCherry;GFP-1

	GFP Signal		
mCherry	No	Chimeric	Normal
High	10	0	0
Medium	0	3	0
Low/No	0	3	5
Total seedlings		21	

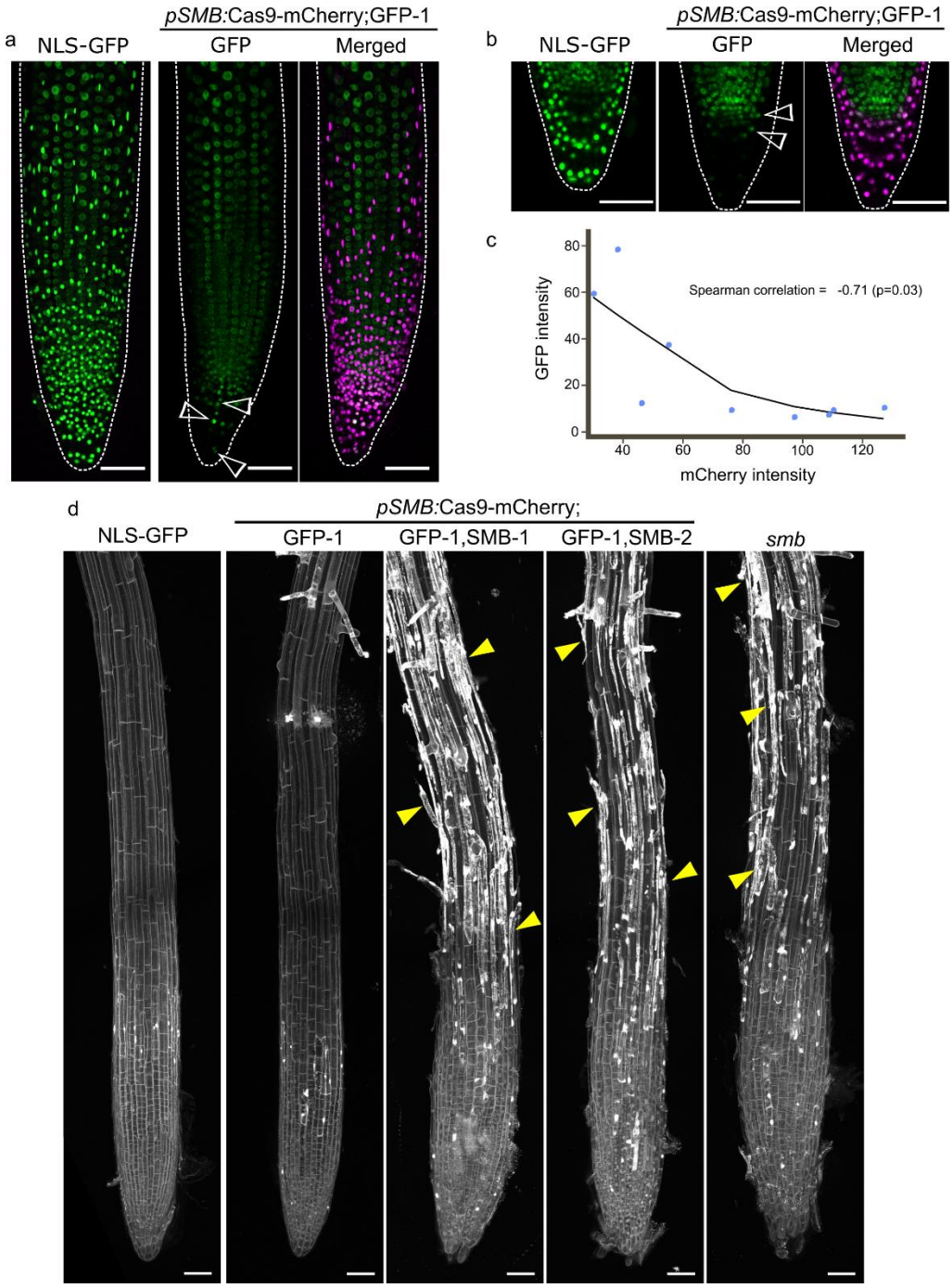

Fig. 2: Root cap specific knockout with CRISPR-TSKO

a, Maximum intensity projection of representative seedling of NLS-GFP, and T1 of *pSMB:*Cas9-mCherry;GFP-1 with absence of GFP and presence of Cas9-mCherry signal specific to root cap cells. GFP is shown in green and Cas9-mCherry in magenta. Arrowheads indicate a patch of root cap cells in which GFP knockout was not achieved (chimera). **b**, Mid-section of root tip of both NLS-GFP and T1 seedling of *pSMB:*Cas9-mCherry;GFP-1. Arrowheads show young root cap cells in which GFP signal can still be observed. **c**, Plot of median intensity of root cap nuclei for both GFP and Cas9-mCherry in T1 seedlings. Line shows a Loess regression curve. **d**, Overview of root tips of 6 DAG T2 seedlings for both gRNAs for *SMB* displaying the characteristic cell corpse accumulation at the root surface (yellow arrowheads) with propidium iodide staining. All scale bars are 50 µm.

To test if a root-cap expressed gene, *SMB* itself, could be successfully targeted by CRISPR-TSKO, the gRNA GFP-1 was combined with one of two different gRNAs targeting *SMB* (SMB-1 and -2) with Cas9 under *pSMB*. The loss of *SMB* activity delays root cap maturation and preparation of programmed cell death in root cap cells, causing larger root caps and a delayed and aberrant root cap cell death with a lack of cell corpse clearance[14]. In CRISPR-TSKO T1 seedlings, we found *smb*-like phenotypes for both independent *SMB* targeting gRNAs coupled with the disappearance of the root cap GFP signal (**Supplementary Fig. 3a**). Both gRNAs appear equally effective as 13 out of 21 and 9 out of 12 T1 events gave clear *smb* and GFP knockout phenotypes, respectively (**Table 2**, **Supplementary Fig. 3a**). The *smb* phenotype and loss of GFP in the root cap cells were also observed in four independent next-generation T2 lines, demonstrating the heritability of CRISPR-TSKO (**Supplementary Fig. 3b**).

Table 2. Phenotypes of T1 seedlings transformed with *pSMB*:Cas9-mCherry;GFP-1,SMB-1 and *pSMB*:Cas9-mCherry;GFP-1,SMB-2

		GFP Signal			*smb* Phenotype		
Vector	mCherry	No	Chimeric	Normal	Yes	Weak	No
GFP-1;SMB-1	High	12 (57%)	0	0	11 (52%)	1 (5%)	0
	Medium	3 (14%)	0	0	1 (5%)	2 (10%)	0
	Low	0	0	2 (10%)	0	0	2 (10%)
	No/Very low	1 (5%)	1 (5%)	2 (10%)	1 (5%)	0	3 (14%)
GFP-1;SMB-2	High	8 (67%)	0	0	7 (58%)	0	1 (8%)
	Medium	0	0	0	0	0	0
	Low	0	3 (25%)	1 (8%)	2 (17%)	0	2 (17%)
	No/Very low	0	0	0	0	0	0

To confirm that the observed phenotypes were due to root cap-specific DNA mutations, root tips from four independent lines (two for each *SMB* target) were protoplasted and used for fluorescence-activated cell sorting (FACS) followed by target sequence

analysis. The mCherry-positive cell populations had indel frequencies >95% for the GFP-1, SMB-1 and SMB-2 target sites, (**Table 3**) as determined by TIDE analysis[22]. In contrast, the mCherry-negative cell populations had indel frequencies of 1-5% which are equivalent to wild-type using this method. Thus the consistent and heritable knockout phenotypes were due to active Cas9-induced mutagenesis specifically in root cap cells.

Table 3. Indel frequencies of T2 protoplasts from root tips

			GFP		*SMB-1*		*SMB-2*	
Line	Targets	Sorted Population	R^2	TIDE Score (%)	R^2	TIDE Score (%)	R^2	TIDE Score (%)
13650.2	*GFP, SMB-1*	mCherry	0.99	99.1	0.98	98.4	-	N.A.
		GFP	0.99	2.9	0.99	5.1	-	N.A.
13650.16	*GFP, SMB-1*	mCherry	0.96	95.4	0.98	98.1	-	N.A.
		GFP	0.99	1.3	1.00	1.3	-	N.A.
13715.5	*GFP, SMB-2*	mCherry	0.97	96.6	-	N.A.	0.97	97.4
		GFP	0.99	3.6	-	N.A.	0.98	2.7
13715.12	*GFP, SMB-2*	mCherry	0.99	98.5	-	N.A.	0.97	96.5
		GFP	0.99	3.1	-	N.A.	0.98	1.1

Cell-lineage-specific gene knockout in stomata

The cis-regulatory promoter elements of *TOO MANY MOUTHS* (*TMM*; AT1G80080) and *FAMA* (AT3G24140) control gene expression during stomata development, with TMM expressing early in the stomatal lineage[23] and FAMA expressing later in the lineage of guard mother cells and young guard cells[24]. These two promoters were used to produce CRISPR-TSKO constructs targeting both GFP and *Phytoene desaturase* (*PDS*; AT4G14210) in the stomatal lineage. PDS is essential for chlorophyll, carotenoid and gibberellin biosynthesis and *pds* null mutants show a dwarfed and photobleached lethal phenotype[25]. Consistent with this, *pPcUbi*:Cas9;GFP-1,PDS vectors targeting *PDS* in a ubiquitous manner gave rise to severe phenotypic effects ranging from full albino to variegated leaves and stunted plants (**Fig. 3a**).

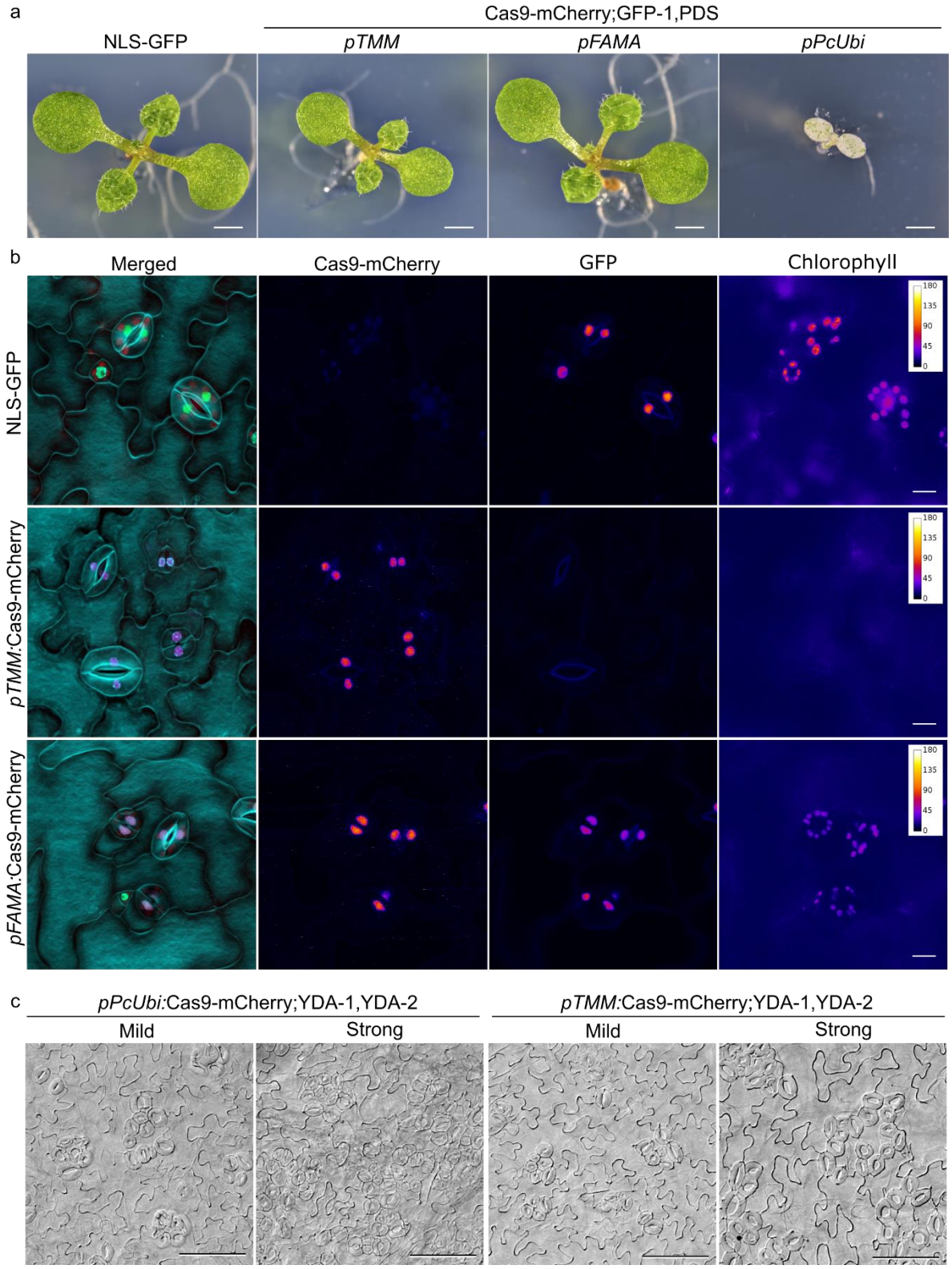

Fig. 3: Stomatal lineage specific knockout with CRISPR-TSKO

a, 9 DAG seedlings showing the partial rescue when *PDS* is knocked out only in stomatal lineage (*pTMM*) in comparison with the arrested albino seedlings of ubiquitous knockout (*pPcUbi*). Scale bars are 1 mm. **b**, Simultaneous stomata lineage specific knockout of GFP and chlorophyll biosynthesis in 5DAG T1

seedlings. Shown are stomata at the abaxial face of cotyledons. While both GFP and chlorophyll signal is lost in stomata in lines under the control of *pTMM*, signal is still present in stomata in lines under the control of *pFAMA*. In merged image, cell outlines are in cyan, GFP in green, Cas9-mCherry in magenta, and chlorophyll autofluorescence in red. Epidermal morphology is shown using DAPI staining. Scale bars are 10 µm. **c**, Targeting of *YDA* only in stomatal lineage (*pTMM*) is sufficient to cause clustering of stomata. Range of stomatal clustering phenotypes is shown on abaxial face of cotyledons of 10 DAG seedlings. Scale bars are 100 µm.

Given the expression patterns of *FAMA* and *TMM*, we expected the *pTMM*-CRISPR-TSKO constructs would show a loss of chlorophyll in all stomata-lineage-derived epidermal cells whereas the *pFAMA*-CRISPR-TSKO constructs should have the knockout phenotype restricted to the late stomatal lineage. At five days after germination, T1 seedlings for both *pTMM*:Cas9-mCherry;GFP-1,PDS and *pFAMA*:Cas9-mCherry;GFP-1,PDS were assessed for the presence of chlorophyll autofluorescence and GFP fluorescence by epifluorescence microscopy. Eighteen out of 20 *pTMM:*Cas9 T1 lines were clearly lacking both GFP and chlorophyll autofluorescence (**Fig. 3b**), indicating highly efficient gene knockout. Intriguingly, restricting the loss of PDS to the stomatal lineage did not markedly affect plant development, as T1 plants were able develop and set seed. Two out of 23 *pTMM:*Cas9 lines did exhibit some mild bleaching similar to the *pPcUbi*:Cas9 events (**Supplementary Fig. 4a**), suggesting that Cas9-mCherry expression from the TMM promoter can leak into mesophyll cells at a low frequency.

In contrast to *pTMM*:Cas9, we observed neither a loss of GFP nor a loss of chlorophyll autofluorescence in any of the 21 mCherry-expressing *pFAMA*:Cas9 T1 seedlings evaluated (**Fig. 3b**). We hypothesized that due to the later induction of Cas9 by *pFAMA*, residual PDS and GFP mRNA and/or protein might still be present in the targeted cells and would have to be depleted before a loss of signal could be observed. Therefore we investigated cotyledons at ten days after germination in five *pTMM:*Cas9 and eight *pFAMA:*Cas9 T1 events. Despite this extended incubation time, mCherry-positive guard cells still showed GFP and chlorophyll signal in the *pFAMA*:Cas9 lines (**Supplementary Fig. 4b).**

To determine if DNA mutations were induced in the *pTMM:*Cas9 and *pFAMA*:Cas9 lines, protoplasts from T2 cotyledons of four independent lines (two for each promoter) were

sorted for mCherry expression. Sequencing results of the mCherry-positive and -negative protoplast populations showed an indel frequency of ~80% for the *GFP* and *PDS* target genes for the *pTMM*:Cas9 lines and 30-74% for the *pFAMA:*Cas9 lines (**Table 4**). The observation of mutations in the *pFAMA:*Cas9 lines was surprising given that no phenotypic effects were observed in any of the events. Despite the lack of phenotypes in the *pFAMA:*Cas9 lines, these results indicate mutations were generated in the mCherry-expressing cells for both CRISPR-TSKO constructs.

Table 4. Indel frequencies of T2 protoplasts enriched for guard cells

				GFP		*PDS*	
Line	Promoter	Targets	Sorted Population	R^2	TIDE Score (%)	R^2	TIDE Score (%)
13651.3	TMM	*GFP, PDS*	mCherry	0.99	78.6	0.96	85.0
			GFP	0.99	0.2	0.98	8.7
13651.10	TMM	*GFP, PDS*	mCherry	0.87	87.0	0.95	73.6
			GFP	0.99	0.5	0.99	6.9
13652.8	FAMA	*GFP, PDS*	mCherry + GFP	0.98	30.0	0.95	74.0
			GFP	0.90	1.5	0.97	8.1
13652.12	FAMA	*GFP, PDS*	mCherry + GFP	0.98	66.3	0.97	47.8
			GFP	0.99	1.3	0.99	6.1

Knockout mutants in *YODA* (*YDA*, AT1G63700) show clustered stomata, severe developmental defects, frequent seedling growth arrest and, if *yda* mutants do manage to survive until flowering, sterility [26, 27]. Given these features, targeting *YDA* specifically in the stomatal lineage with *pTMM*-CRISPR-TSKO presents a perfect test case. When targeted by ubiquitously-expressed Cas9 by a dual-gRNA construct, *pPcUbi*:Cas9-mCherry;YDA-1,YDA-2, 33 out of 35 mCherry-positive T1 seedlings contained clustered stomata on the cotyledonary abaxial epidermis to varying degrees of severity (**Fig. 3c**). Strikingly, all 40 mCherry positive T1 plants carrying *pTMM*:Cas9-mCherry;YDA-1,YDA-2 copied this stomata phenotype.

Remarkably, in contrast to the *pPcUbi:Cas9* lines, the *pTMM:Cas9* lines developed similar to the wild type. From a separate batch of T1 plants transferred to soil, all 19

pTMM:Cas9 T1 plants were fertile and set seed while 8 out of 19 *pPcUbi*:Cas9 lines were completely sterile. PCR and DNA sequence analysis confirmed efficient mutagenesis at the YDA target sites in whole seedlings transformed with both constructs. As a pair of gRNAs are used to target YDA, an 813 bp deletion is expected from the excision of the intervening DNA sequence. Such deletion events are observed for both constructs (**Supplementary Fig. 4c**). Indel frequencies for *pPcUbi*:Cas9-mCherry;YDA-1,YDA-2 events were higher than *pTMM*:Cas9-mCherry;YDA-1,YDA-2 events as is expected for ubiquitous versus stomata-specific targeting.

These results illustrate that by utilizing the stomatal lineage-specific *TMM* promoter, we were able to uncouple the pleiotropic growth defects and sterility in systemic *YDA* knockouts[27], but still retain the characteristic clustered-stomata phenotype and obtain T2 seeds.

Organ-specific gene knockout in lateral roots

Next to specific gene-knockout in particular tissues and cell lineages, we tested the potential of CRISPR-TSKO to generate entire mutant organs on otherwise wild-type plants. To this end we made use of the promoter sequence of *GATA23,* a gene that marks the initiation of lateral root organogenesis and is expressed in pericycle cells primed to become involved in lateral root formation in Arabidopsis[28]. *GATA23* expression is transient and disappears prior to the emergence of the primordium from the primary root, except for some remaining expression at the base of the primordium[28] (**Fig. 4a**). Strikingly, 20 out of 23 mCherry-positive T1 seedlings carrying *pGATA23:*Cas9-mCherry;GFP-1 showed a complete or partial loss of GFP fluorescence in lateral roots, while maintaining normal GFP expression in the primary root (**Table 5, Fig. 4a,b**). Lines with undetectable mCherry expression showed chimeric or normal expression patterns in lateral roots (**Table 5**). Sequence analysis of lateral roots from six independent events confirmed >94% of the alleles were mutated in these organs (**Table 6**). These results indicate that organ-specific gene knockout in lateral roots is feasible via the lateral root founder cell-expressed *GATA23* promoter.

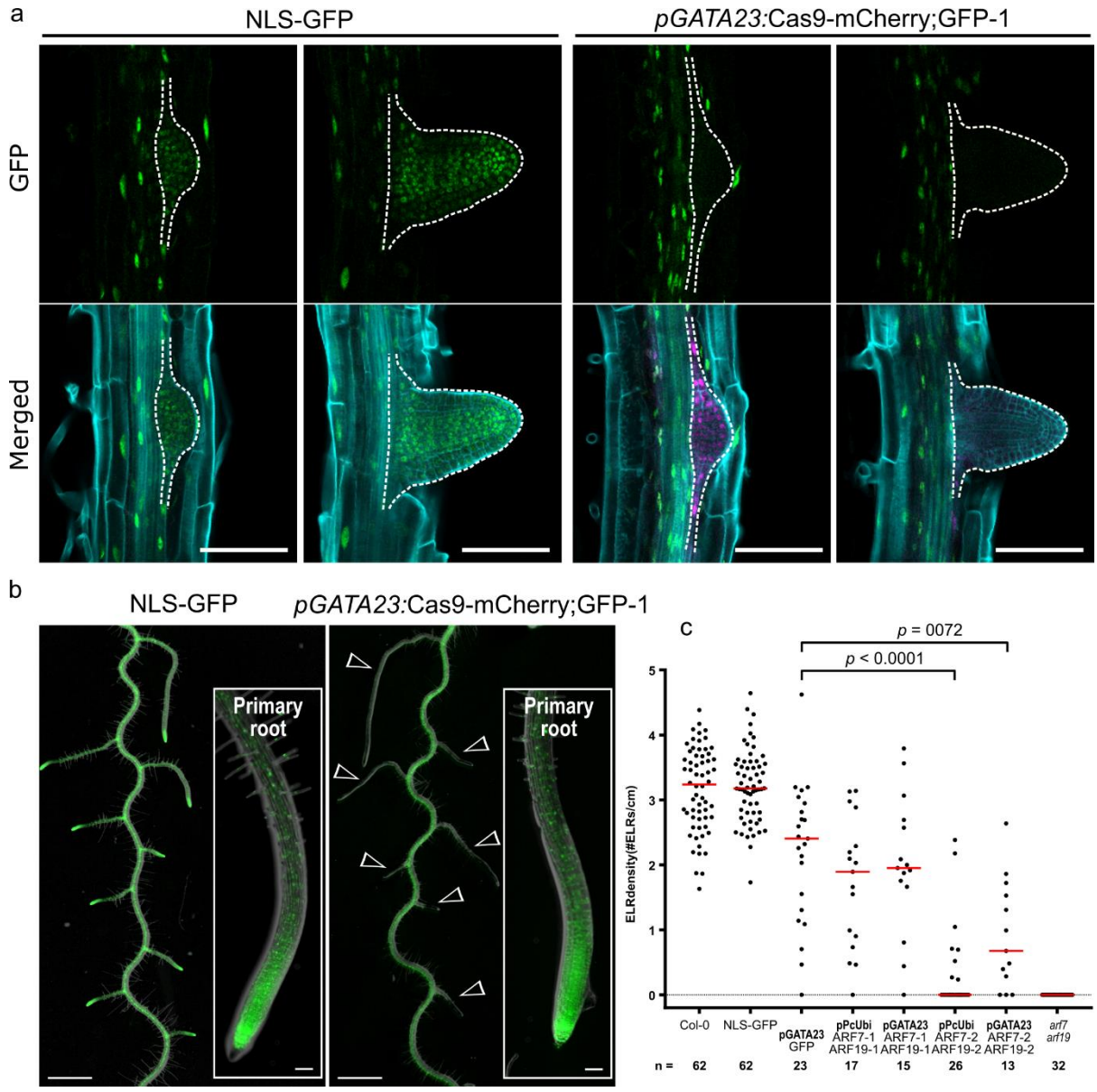

Fig. 4: Organ specific gene knockout using pGATA23-CRISPR-TSKO

a, Specific knockout of the GFP signal in emerging later roots (dashed outline). Representative images of the NLS-GFP control and *pGATA23*:Cas9-mCherry;GFP-1. GFP in green, mCherry in magenta, and cell wall stained with calcofluor white in cyan. Scale bars are 100 µm. **b**, GFP knockout is specific to lateral roots. Overlay of root morphology and GFP signal is shown fora representative NLS-GFP control and a T2 *pGATA23*:Cas9-mCherry;GFP-1seedling. Arrowheads indicate GFP negative lateral roots. Insets are the tip of primary roots. Scale bars are 1 mm for overview and 100µm for inset. **c**, Quantification of the emerged lateral root (ELR) density for Col-0, NLS-GFP, T1 seedlings of *pGATA23*-CRISPR-TSKO, and *arf7arf19* knockout line. The median of the population is indicated with a red bar. Kruskal-Wallis test ($p < 0.0001$) followed by Dunn's multiple comparisons test was conducted to compare ELR density of T1 seedlings of CRISPR-TSKO with *pGATA23:*Cas9-mCherry;GFP-1 seedlings. *p* values smaller than 0.09 are shown.

Table 5. GFP phenotype in lateral roots of *pGATA23*:Cas9-mCherry;GFP-1

	GFP Signal		
mCherry	No	Chimeric	Normal
Positive	15	5	3
Negative	0	3	27
Total seedlings	15	8	30

Table 6. Indel frequencies of individual *pGATA23*:Cas9-mCherry;GFP-1 T1 lines

T1 Line	Targets	mCherry expression	GFP phenotype in LR	R^2	TIDE Score (%)
4	GFP-1	Positive	KO	0.99	96.9
5	GFP-1	Positive	KO	0.99	96.4
6	GFP-1	Positive	Chimeric	0.93	29.4
7	GFP-1	Negative	WT	0.99	3.2
30	GFP-1	Positive	KO	0.98	93.7
31	GFP-1	Negative	WT	0.99	1.7
32	GFP-1	Positive	KO	0.96	96.3
33	GFP-1	Positive	KO	0.99	95.3
34	GFP-1	Positive	KO	0.98	93.0

To test the *pGATA23*-CRISPR-TSKO construct on genes involved in lateral root formation, the auxin-response factors *ARF7* (AT5G20730) and *ARF19* (AT1G19220) were targeted. Lateral root organogenesis depends on the partially redundant action of *ARF7* and *ARF19* as *arf7 arf19* double-knockout mutants are not able to develop lateral roots[29]. As both ARFs are broadly expressed in Arabidopsis seedlings, it is unknown whether this phenotype depends on ARF7 and ARF19 function strictly in pericycle cells[30]. To test this, we first recapitulated the systemic knockout of ARF7 and ARF19 in T1 plants with two ubiquitously-expressed Cas9 vectors containing two gRNAs targeting both ARFs, *pPcUbi*:Cas9-mCherry;ARF7-1,ARF19-1 and *pPcUbi*:Cas9-mCherry;ARF7-2,ARF19-2. Consistent with the published phenotype of *arf7 arf19* double mutant[30], a significant reduction in lateral root density was observed for *pPcUbi*:Cas9-

mCherry;ARF7-2,ARF19-2 T1 plants compared to *pGATA23:*Cas9-mCherry;GFP-1 T1s with 18 out of 26 T1 plants completely lacking lateral roots (**Fig. 4c**). No reduction in lateral root density was observed for the *pPcUbi*:Cas9-mCherry;ARF7-1,ARF19-1 T1s. In agreement with these phenotyping results, sequencing of the gene target sites in whole roots from four independent events showed the indel frequency was >93% for most events with the *pPcUbi*:Cas9-mCherry;ARF7-2,ARF19-2 vector (**Table 7**). The *pPcUbi*:Cas9-mCherry;ARF7-1,ARF19-1 construct was particularly ineffective as the ARF19-1 target site had a low indel frequency of only 9-13% (**Table 7**), and explaining the lack of mutant phenotype in those T1s.

Table 7. Indel frequencies of individual *pPcUbi*:Cas9-mCherry;ARF7-1,ARF19-1 and *pPcUbi*:Cas9-mCherry;ARF7-2,ARF19-2 T1 lines

			ARF7		*ARF19*	
Sample	Targets	mCherry expression	R^2	TIDE Score (%)	R^2	TIDE Score (%)
8	ARF7-1, ARF19-1	Positive	0.87	62.0	0.99	8.9
9	ARF7-1, ARF19-1	Positive	0.99	24.5	0.99	3.0
10	ARF7-1, ARF19-1	Positive	0.98	20.7	0.99	2.8
11	ARF7-1, ARF19-1	Positive	0.92	62.7	0.99	13.2
NLS-GFP			0.98	4.2	0.99	1.0
12	ARF7-2, ARF19-2	Positive	0.96	95.2	0.99	97.9
13	ARF7-2, ARF19-2	Positive	0.95	94.6	0.94	93.2
14	ARF7-2, ARF19-2	Positive	0.91	72.3	0.99	98.9
15	ARF7-2, ARF19-2	Negative	0.99	0.3	0.99	0.9
NLS-GFP			0.99	2.3	0.99	0.8

By targeting *ARF7* and *ARF19* in the xylem-pole pericycle via the *pGATA23*:Cas9-mCherry-ARF7/ARF19-2 construct, a significant reduction in lateral root density was also observed and 3 out of 13 T1 seedlings produced no lateral roots (**Fig. 4c**). These results show that CRISPR-TSKO can efficiently knock out two genes at once in lateral root founder cells, and that ARF7 and ARF19 action specifically within the GATA23-expressing xylem-pole pericycle is required for lateral root formation.

Discussion

Conditional knockout of essential genes enables their study in specific contexts

Targeted gene knockout experiments in plants typically have the objective of generating stably transmitted, inheritable DNA mutations. The generation of such knockout lines is a powerful tool for the functional analysis of many genes of interest. However, this approach is difficult to apply to genes that are essential for cell survival or reproduction, or those that have severe pleiotropic effects when mutated. In cases of lethality or sterility, such alleles need to be maintained in a heterozygous state[31]. Moreover, context-specificity of key regulators of developmental processes is often taken for granted without further experimental proof, while being aware of the non-context specific expression. In this report we describe the design and validation of CRISPR-TSKO, a gene knockout approach in plants that can be used to overcome these limitations.

We targeted six genes using four different tissue-specific promoters. Two of the target genes, *PDS* and *YDA*, are essential for plant growth and development. Mutations in *PDS* induced with the *pTMM:*Cas9-mCherry;GFP-1,PDS vector led to the expected defects in chlorophyll content and chloroplast formation[25] specifically in the stomatal lineage. Importantly, the active photosynthetic mesophyll tissue was not markedly affected in non Cas9-expressing cells which allowed these plants to develop as vigorously as the wild type (**Fig. 3a, Supplementary Fig. 4a**). This stands in contrast to the ubiquitous CRISPR knockout lines that were primarily dwarfed albino plants not viable in soil.

In wild-type Arabidopsis, chlorophyll-containing chloroplasts are formed in epidermal pavement as well as stomatal guard cells, though they are much smaller than mesophyll chloroplasts[32]. The function of chloroplasts in guard cells has been subject to debate[33]. Very recently, the discovery of the *gles1* (*green less stomata 1)* mutant suggests that functional chloroplasts in guard cells are important for stomatal responses to CO_2 and light, resulting in stomatal opening[34]. CRISPR-TSKO plants with mutated PDS specifically in the stomatal lineage represent a powerful resource to test these and other hypothesized functions of chloroplasts in guard cells.

The mitogen-activated protein kinase YDA has several roles during plant development including embryogenesis, epidermal patterning and root development[35, 36]. Accordingly, *yda* mutants have severe pleiotropic phenotypes. Already directly after fertilization, *yda* mutants fail to establish the first asymmetric division of the zygote and ensuing embryo development is severely compromised[27]. Some *yda* embryos do continue to develop into seedlings, but these rarely survive on soil and the few *yda* plants that flower are severely dwarfed and completely sterile[26, 27].

Using CRISPR-TSKO to target *YDA* only in the stomatal lineage, all transgenic events expressed a range of clustered stomata *yda* phenotypes while the other aspects of plant development were not notably compromised. Critically, all lines transferred to soil were fertile. These results demonstrate how CRISPR-TSKO can facilitate the analysis of gene function in specific developmental contexts, and it shows that *YDA* function in the stomatal lineage can be uncoupled from the pleiotropic defects caused by *YDA* mutations in other developmental contexts.

The root cap is a particularly interesting plant tissue as it encompasses all stages of plant cellular life – generation by stem cells, proliferation, differentiation, and finally programmed cell death and separation – in a compact spatial and temporal frame of a few hundred microns and a couple of days[37]. In this light, the *pSMB*-CRISPR-TSKO vector system could particularly useful to study genes essential for basic cellular functions in an easily accessible root tissue.

SMB is a key transcription factor required for root cap maturation and programmed cell death and its expression starts immediately after the formative stem cell division in the root cap daughter cells[13, 14]. Our results show that *pSMB*-CRISPR-TSKO allows gene knockout in new root cap cells from the moment of their inception. Diminishing GFP fluorescence is detectable in the two youngest root cap layers (**Fig. 2a,b**). This is likely due to remaining pools of mRNA and protein that have to be turned over before the GFP loss-of-function phenotype becomes apparent. The speed of these processes likely depends of the stability of the particular mRNA and protein, or even the cell type in question. The results presented here highlight that these dynamics have to be taken into

account on a gene-by-gene and tissue-specific promoter basis when designing and analyzing tissue-specific gene knockout experiments.

Organ-specific knockout

In the case of the stomatal lineage and the root cap, specific cell types and tissues were targeted by CRISPR-TSKO, whereas in our lateral root experiments, we targeted the organ primordial founder cells to generate entirely mutated lateral roots. The generation of completely GFP-negative lateral roots at high rates impressively shows the efficiency of CRISPR-TSKO under *pGATA23*. Having a promoter at hand that is activated in the founder cells of a new organ thus represents an effective means to generate whole organs devoid of the function of a gene of interest. This experimental approach is an attractive alternative to grafting to study the transmission of mobile signals such as small RNAs[38]. Moreover, essential genes for primary root development such as *MONOPTEROS* hinder loss-of-function analysis during lateral root development[39]. The *pGATA23*-CRISPR-TSKO will enable us to uncouple the function of such genes involved in primary- and lateral root development.

Plants possess a modular body structure and a high regenerative potential. Thus, mutated lateral roots can be used to generate entire plants via shoot regeneration culture[40]. In that way, above-ground organs could be investigated for phenotypes generated by lateral-root CRISPR-TSKO. We observed a strong correlation between gene knockout and Cas9-mCherry expression, which can be used to facilitate selection of mutated lateral roots. Furthermore, targeting of GFP alongside a gene of interest in a ubiquitously-expressing NLS-GFP background revealed that knockout of GFP strongly correlated with mutagenesis of the endogenous genes *SMB* and *PDS*. Thus, both tagged Cas9 as well as knockout of reporter genes facilitate the selection of successful CRISPR knockout events in tissues and organs.

CRISPR-TSKO; A powerful and versatile tool

To facilitate the construction of CRISPR-TSKO reagents, we developed a modular vector-cloning scheme based on the GreenGate system[17]. The modularity of the cloning system allows for the rapid assembly of new promoter sequences with Cas9 or any

nuclease of choice. Targeting specificity in spatial and temporal contexts can be readily achieved with the recently-developed inducible and tissue-specific plant expression systems that utilize GreenGate technology[41]. The cloning reagents used here are inexpensive to use and can be readily adopted by any laboratory. The system can be easily expanded to accommodate up to twelve gRNAs by the use of an AarI-*SacB* linker and later additions of six paired-gRNA entry modules (**Supplementary Fig. 2 and Supplementary Methods**). For ease of use, a workflow was developed to substitute the AarI restriction sites in the AarI linker for BsaI restriction sites flanking the *ccd*B and *Cm*R selectable markers (**Fig. 1 and Supplementary Fig. 2**). This strategy avoids the need for separate AarI digestions of regularly-used destination vectors and provides a negative selection marker for the original destination vector in *ccd*B sensitive cells (*e.g.* DH5α). Alternatively, additional expression cassettes can be sequentially inserted into the AarI-*SacB* or BsaI-*ccdB* linkers. Hence, the system presented here can be easily used and modified for a variety of applications.

One general characteristic of CRISPR-TSKO is the continuous *de-novo* generation of mutations in cells that start to express Cas9. In the case of the root cap, every formative stem cell division creates a novel gene knockout event. In the stomatal lineage, every cell that starts expressing TMM or FAMA generate independent mutations, and in the case of the lateral root, every GATA23-expressing founder cell will contribute individual mutations to the lateral root primordium. All cells the lateral root primordium go back to a small number of founder cells, each of which is responsible for the formation of a portion of the lateral root primordium[42].

Most gene mutations lead to small indels causing frame shifts and early stop codons, but a few should also lead to in-frame mutations, thereby disturbing the eventual amino-acid sequence of the protein only minimally. The GFP-1 gRNA used here targets the essential Gly67 residue, so that even in-frame mutations are likely to result in a loss of fluorescence[43]. Hence, gRNAs targeting genes of interest in particularly sensitive sites, as crucial interaction domains or active sites can further increase the effectiveness of CRISPR-TSKO.

Based on the results of this study, we suggest several tissue-specific promoters be tested before more labor-intensive phenotyping is performed for genes of interest. This test can simply be performed by analyzing the ubiquitously expressing NLS-GFP plant line transformed with the gRNA GFP-1 under the control of a new promoter of choice. This approach clearly demonstrated the context-specific knockout with the *SMB*, *TMM*, and *GATA23* promoters. However, results might not always be straightforward as clearly illustrated with the *FAMA* promoter. The use of this promoter did not result in an observable phenotype while DNA mutations were detected. Therefore, ideally more than one promoter should be tested when targeting novel cell types with CRISPR-TSKO.

In conclusion, cell type-, tissue-, or organ-specific gene knockout by targeted expression of Cas9 is a powerful means of functional analysis in specific spatial and temporal contexts of plant development. Especially if genes are widely expressed or have fundamental roles for cell survival or plant reproduction, CRISPR-TSKO allows for the generation of stable transgenic lines that target mutagenesis specifically to the cell, tissue or organ of interest. Unlike in system-wide, heritable mutant approaches, no defined mutant alleles are generated. Nevertheless, due to the high efficiency of CRISPR mutations causing loss of gene function, heritable expression of CRISPR-TSKO provides a powerful tool to detect and analyze phenotypes in specific cellular or tissular contexts. As with other CRISPR applications, CRISPR-TSKO is forward-compatible to incorporate upcoming future variations of CRISPR gene modification. Together with the virtually unlimited possibilities to combine different promoters, reporters, or tags in CRISPR-TSKO, this technology presents a powerful addition to the molecular genetics tool-box in plant biology research.

Distribution of modules, plasmids, and protocols

All cloning modules and plasmids reported here are available via the VIB-UGent Center for Plant Systems Biology Gateway Vector website (**Supplementary Table 1**; https://gateway.psb.ugent.be/search). See **Supplementary methods** for detailed cloning protocols.

Seeds for the pHTR5:NLS-GUS-GFP line are available upon request.

Methods

Cloning

All cloning reactions were transformed via heat-shock transformation into *ccdB*-sensitive DH5α *E. coli* or One Shot™ *ccd*B Survival™ 2 T1R Competent Cells (ThermoFisher Scientific). Depending on the selectable marker, the cells were plated on LB medium containing 100 µg/mL carbenicillin, 100 µg/mL spectinomycin, 25 µg/mL kanamycin or 10 µg/mL gentamycin. Colonies were verified via colony-touch PCR, restriction digest and/or Sanger sequencing by Eurofins Scientific using the Mix2Seq or TubeSeq services. All cloning PCR reactions were performed with either Q5® High-Fidelity DNA Polymerase (New England Biolabs) or iProof™ High-Fidelity DNA Polymerase (BioRad Laboratories). Gibson assembly reactions were performed using 2x NEBuilder Hifi DNA Assembly Mix (New England Biolabs). Column and gel purifications were performed with Zymo-Spin™ II columns (Zymo Research).

Golden Gate entry modules

Golden Gate entry modules were made by PCR amplification of gene fragments and inserting the purified PCR product into BsaI-digested GreenGate entry vector[17] via restriction-ligation using BsaI (New England Biolabs) or Gibson assembly. See **Supplementary Table 3** for all primers used. The entry modules pGG-F-AarI-AarI-G and pGG-F-AtU6-26-AarI-AarI-G were made by annealing oligos 361 and 362 and ligating into the BsaI-digested entry vector pGGF000. The Golden Gate entry linker modules were constructed as previously described[44]. The AarI-SacB-AarI linker, based on the SacB sequence from pMA7-SacB[45], was synthesized on the BioXP3200 DNA synthesis platform (SGI-DNA) and inserted into a BsaI-digested pGGF000 plasmid via Gibson assembly. The correct clone was verified by Sanger sequencing. The coding sequence for mTagBFP2, based on a previously reported mTagBFP2[46], was PCR amplified with primers RB42 and RB43 from a synthesized fragment (Gen9) and inserted into a BsaI-digested pGGC000 plasmid via restriction ligation.

The unarmed gRNA modules were cloned by amplifying the AtU6-26 promoter and gRNA scaffold from previously-described Golden Gate entry vectors[44]. The amplification

was done using the forward primer 120 and the reverse primers 283, 284, 230, 231, 232 and 233 for the B to G overhangs, respectively. This removed an unwanted attB2 site. PCR products were digested with BsaI and ligated into the respective empty entry vectors. The unarmed gRNA modules were further adapted by adding the *ccdB* negative selectable marker. The *ccdB* gene was PCR amplified from pEN-L1-AG-L2 with oligos 391 and 392 and inserted into BbsI-digested unarmed gRNA modules via Gibson assembly. All clones were verified by Sanger sequencing.

GATEWAY™ destination vectors

pGG-A-pOLE1-B, pGG-B-OLE1-C, pGG-D-linker-E[17], pGG-E-NOST-F and pGG-F-LinkerII-G were assembled with either pGG-C-mRuby3-D or pGG-C-GFP-D[17] into pEN-L1-A-G-L2. The ligation reactions were used as templates for PCR with the primers 195 and 196. The PCR products were cloned via Gibson assembly into pGGK7m24GW linearized with KpnI and XbaI. Clones were verified by Sanger sequencing. The resulting vectors containing the red and green fluorescent FAST markers were named pFASTRK24GW and pFASTGK24GW, respectively.

Proof-of-concept vectors

The Golden Gate entry modules pGG-A-*pSMB*-B, pGG-B-Linker-C, pGG-C-Cas9PTA*-D, pGG-D-Linker-E, pGG-E-G7T-F and pGG-F-linkerII-G were assembled in pEN-L4-A-G-R1[44], resulting in the vector pEN-L4-*pSMB*-Cas9PTA-G7T-R1. The Golden Gate entry module pGG-A-AtU6-26-BbsI-BbsI-B and pGG-B-linkerII-G were assembled in pEN-L1-A-G-L2[44], resulting in the vector pEN-L1-AtU6-26-BbsI-BbsI-L2. The BbsI restriction sites were swapped with a fragment containing the *ccdB* and *CmR* selectable markers flanked with BsaI sites. This fragment was PCR amplified from the plasmid pEN-L4-A-G-R1, using primers 1436 and 1437. The fragment was BsaI-digested and ligated with T4 DNA Ligase in the BbsI-digested vector pEN-L1-AtU6-26-BbsI-BbsI-L2, resulting in the vector pEN-L1-AtU6-26-BsaI-BsaI-L2. pEN-L4-*pSMB*-Cas9PTA-G7T-R1 and pEN-L1-AtU6-26-BsaI-BsaI-L2 were recombined in pGGB7m24GW[47] via a MultiSite Gateway reaction according to manufacturer's recommendations. This vector was called pB-*pSMB*-Cas9-G7T-AtU6-BsaI-BsaI-gRNA scaffold.

Oligos 138 and 139 (GFP-1 target) and oligos 134 and 135 (GFP-2 target) were annealed by adding 1 µL of each 100 µM oligonucleotide in 48 µL of MQ and incubating with a slow cooling program on the thermal cycler (5 minutes at 95°C; 95-85°C, -2°C/second; 85-25°C, -0.1°C/second). These annealed oligonucleotides were cloned via a Golden Gate reaction into pB-*pSMB*-Cas9-G7T-AtU6-BsaI-BsaI-gRNA scaffold. The Golden Gate reaction conditions are described in **Supplementary Methods**. The resulting vectors were named pB-*pSMB*-Cas9-G7T-AtU6-GFP-1 and GFP-2.

Golden Gate destination

The Golden Gate destination vectors were cloned by amplifying the *CmR* and *ccdB* selection cassettes, flanked by the Golden Gate cloning sites A-G, from pEN-L1-A-G-L2 using primers 298 & 313. PCR products were column purified and cloned via Gibson assembly in the HindIII and PstI linearized Gateway destination vectors pGGP7m24GW, pGGK7m24GW, pGGB7m24GW, pGGPH7m24GW[47], pFASTRK24GW and pFASTGK24GW. The resulting vectors were named respectively pGGP A-G, pGGK A-G, pGGB A-G, pGGH A-G, pFASTRK A-G, pFASTGK A-G. All clones were verified by Sanger sequencing and diagnostic digest with NotI.

To generate the pFASTR-A-G destination vector, the Golden Gate entry modules pGG-A-OLE1P-B, pGG-B-OLE1-CDS-C, pGG-C-mRuby3-D, pGG-D-Linker-E, pGG-E-NOST-F, pGG-F-linkerII-G were assembled in pGGP-A-G. Subsequently the *CmR* and *ccdB* selection cassettes, flanked by the Golden Gate cloning sites, were PCR amplified using primers 298 and 430 from pEN-L1-AG-L2 and inserted via Gibson assembly.

One-step CRISPR-TSKO cloning vectors

For cloning two gRNAs in a destination vector, we followed as similar approach as previously described[48], with some modifications. A plasmid was generated to serve as a PCR template for 2-gRNA vectors. The Golden Gate entry modules pGG-A-AtU6-26-BbsI-BbsI-B, pGG-B-Linker-C[17], pGG-B-AtU6PTA-C[44] and pGG-D-linkerII-G were assembled in pEN-L1-A-G-L2 to generate pEN-2xAtU6 template. The clone was verified by Sanger sequencing.

The extended protocol for making one-step, CRISPR-TSKO cloning vectors can be found in **Supplementary Methods**. In summary, six different entry modules are combined via Golden Gate assembly in a destination vector. The A-B entry module contains the tissue-specific promotor, the C-D module contains the Cas9 endonuclease and can be combined with an N-terminal tag (B-C) or C-terminal tag (D-E), and the E-F entry module contains the terminator. For making a vector that is compatible with cloning one or two gRNAs, the F-G module pGG-F-AtU6-26-AarI-AarI-G is used (**Fig. 1**). Upon digestion with AarI, this vector can be loaded directly with one or two gRNAs. Alternatively, the AarI sites can be replaced for a fragment containing BsaI sites flanking the *ccdB* and *CmR* selectable markers. Two gRNAs can be cloned via a PCR reaction on the pEN-2xAtU6 template using primers that contain gRNA spacer sequences via a Golden Gate reaction. More details can be found in **Supplementary Methods**.

For making a vector that is compatible with multiple gRNA's (up to 12) the Golden Gate cloning is slightly modified. The initial Golden Gate reaction is performed with an F-G linker containing AarI restriction sites (**Supplementary Fig. 1**). Upon AarI digestion, this vector can be directly loaded with six Golden Gate entry modules containing one or two AtU6-26 promotors and gRNAs. Alternatively, a similar strategy to replace the AarI sites by the *ccdB* and *CmR* selectable markers flanked with BsaI sites can be followed.

Plant lines used in this study

The *smb-3* line is derived from the SALK collection (SALK_143526C). The NLS-GFP line (pHTR5:NLS-GUS-GFP) was previously reported[15]. The *arf7 arf19* double mutant[30] is derived from the ABRC collection (CS24629).

Plant transformation

Plant vectors were transformed in *Agrobacterium tumefaciens* C58C1 by electroporation. Transformation in pHTR5:NLS-GUS-GFP via the floral dip method[49]. For constructs containing the bar selectable marker or FASTR screenable marker, the T1 seed selection was done on 1/2 MS medium + 10 mgL^{-1} Glufosinate-ammonium (Sigma-Aldrich) or by selection under a Leica M165FC fluorescence stereomicroscope.

Resistant seedlings or pFASTR-positive seeds were transferred to Jiffy-7 pellets® and grown in a greenhouse at 21°C under a 16-hour day regime.

DNA extraction and molecular analysis

Seedling, leaves or roots were frozen and disrupted to powder using a TissueLyser (Retsch MM300). DNA was extracted using a modified version of the protocol from Edwards et al. (1991 Nucleic Acids Research 19:1349). The modifications consisted of an adapted extraction buffer (100 mM Tris HCl pH 8.0, 500 mM NaCl, 50 mM EDTA, 0.7% SDS) and a 70% ethanol washing step before dissolving the pellet. A region around the CRISPR/Cas9 target site was PCR amplified using the ALLin™ Red Taq Mastermix, 2X (highQu GmbH) with the following program on the thermocycler: 95°C for 3 minutes, followed by 33 cycles (30 seconds at 95°C, 30 seconds at the annealing temperature, 1 minute/kb at 72°C), 72°C for 5 minutes. The PCR products were analyzed via agarose gel electrophoresis and the clean-up was either done by bead purification with HighPrep^{TM} PCR (MAGBIO) or column purification with the DNA Clean & Concentrator^{TM} kit (Zymo Research). The purified samples were send for Sanger sequencing (Eurofins Scientific) and analyzed using TIDE[22].

All gRNA target sites can be found in **Supplementary Table 2**.

Confocal microscopy for original proof of concept

T1 seedlings were imaged on a Zeiss LSM710 confocal microscope. GFP was excited at 488nm and acquired between 500-550nm. T2 seedlings were imaged on a Leica SP8X confocal microscope. GFP was excited at 488nm and acquired between 500-530nm.

Confocal microscopy

Seedlings were imaged on a Leica SP8X confocal microscope. For root imaging, GFP was excited at 488nm and acquired between 500-530nm. mCherry was excited at 594nm and acquired between 600-650nm. Samples were either stained with 20ug/mL of DAPI or with 10µg/mL of propidium iodide in 0.43gL^{-1} Murashige and Skoog salts with 94µM MES.H_2O medium. DAPI was excited at 405nm and acquired between 410-480nm in sequential mode.

For stomata imaging, cotyledons were vacuum infiltrated with with 20ug/mL of DAPI in 0.43gL^{-1} Murashige and Skoog salts with 94µM MES.H_2O medium. Samples were imaged in sequential mode. DAPI was excited at 405nm and acquired between 410-450nm. GFP was excited at 488nm and acquired between 500-530nm. mCherry was excited at 594nm and acquired between 600-650nm. Chlorophyl autofluorescence was excited at 488nm and acquired between 680-730nm. Images were analyzed using Fiji[50].

To image lateral root primordia, T1 seedlings were cleared using the ClearSee protocol[51, 52] in combination with cell wall staining using Calcofluor White M2R (Sigma) on a Leica SP8X confocal microscope. Calcofluor White was excited at 405nm and acquired between 430-470nm. GFP was excited at 488nm and acquired between 500-525nm. mCherry was excited at 594nm and acquired between 600-630nm.

Epifluorescence microscopy

Cotyledons of FASTR positive seedlings were mounted on distilled water and observed on a Zeiss Observer.Z1 using a Plan-Apochromat 20x/0.8 DICII objective. GFP fluorescence was observed with a BP 470/40 filter for excitation, a FT 495 beam splitter, and a BP 525/50 emission filter. mCherry was observed with a BP 545/25 filter for excitation, a FT 570 beam splitter, and a BP605/70 emission filter.

Segmentation and analysis of root cap nuclei

Root tip image stacks were segmented and nuclei intensity measurements performed using the interactive learning and segmentation toolkit ilastik 1.3.0[53]. Intensity of GFP and mCherry were measured for segmented nuclei with a probability equal or higher than 0.95 of belonging to root cap cells. Based on mCherry measurements in the NLS-GFP line (**Supplementary Fig. 5**), a threshold of 25 was established as a minimum signal for mCherry.

Protoplast preparation and cell sorting

Protoplasting was performed as previously described[54]. Briefly, for *pSMB*-CRISPR-TSKO lines, root tips of 5 day old seedlings grown under continuous light on 0.43gL^{-1} Murashige and Skoog salts with 94µM MES.H_2O medium were incubated in

protoplasting solution consisting of 1.25% cellulase (Yakult, Japan), 0.3% Macerozyme (Yakult, Japan), 0.4M mannitol, 20mM MES, 20mM KCl, 0.1% BSA and 10mM $CaCl_2$ at pH 5.7 for 3 hours. Samples were then filtered through a 40µm filter and the flow through centrifuged at 150xg for 10min. Supernatant was discarded and protoplasts were recovered in ice-cold resuspension buffer. Resuspension buffer was of same constitution as protoplasting buffer with the omission of both cellulase and macerozyme. For lines targeting stomatal lineages, cotyledons of 5-day old seedlings were processed as above but with a 12 hours incubation time to get proper release of guard cells.

Root tip protoplasts were sorted into 1.5ml Eppendorf tubes containing 500µl of resuspension buffer using a BD FACSAriaII, equipped with 3 lasers (405nm, 488nm and 633nm). To account for the double presence of GFP and mCherry in some samples, the cotyledon protoplasts were sorted into 1.5ml Eppendorf tubes containing 500µl of resuspension buffer using a BD FACSMelody, equipped with 3 lasers (405nm, 488nm and 561nm). The 561nm laser in the BD FACSMelody made a better separation possible due to a better excitation of the mCherry. All FACS sorting reports can be found in **Supplementary Fig. 6**.

Quantification of lateral root density

FASTR positive seeds were sown on half-strength Murashige and Skoog (MS) medium (Duchefa Biochemie B.V.), supplemented with 1% (w/v) sucrose and 0,8% (w/v) agar, at pH 5,7 and stratified for 2 days in the dark at 4°C. Seedlings were grown vertically for 12 days in continuous light (100 µmol $m^{-2}s^{-1}$) at 22°C. Presence/absence of Cas9-mCherry signal was scored using a Leica M165FC fluorescence stereomicroscope. The number of emerged lateral roots was determined for every seedling using a stereo microscope and root lengths were measured via Fiji[50] using digital images obtained by scanning the petri dishes.

Stomata analysis of cotyledons in *YDA* targeting lines

The cotyledon epidermis of seedlings 10 days post germination was visualized by clearing cotyledons in 100% ethanol and incubation at 60 degrees in 90% ethanol / 10% acetic acid for 30 minutes and ethanol / 1,25M sodium hydroxide (1:1 v/v) for 2 hours.

Next, cotyledons were incubated overnight at room temperature in lactic acid saturated with chloral hydrate, washed in 100% lactic acid and mounted for differential interference contrast microscopy (Olympus BX51). Images (430 µm x 566 µm) from the midline to the margin on abaxial surfaces were generated. Thirty five to 40 cotyledons of individual seedlings were evaluated per genotype.

Statistical analysis

For segmentation and analysis of root cap nuclei, Spearman's Correlation Coefficient between median root cap signal of GFP and mCherry was calculated using SAS (Version 9.4M5 of the SAS System for windows 7 64bit. Copyright © 2013 SAS Institute Inc. Cary, NC, USA (www.sas.com)). The SAS code is available upon request. For lateral root density analysis, statistical significance was assessed using the Graph-Pad Prism software, version 7.03 (GraphPad Software, Inc.). The comparison of ELR densities for different constructs was done using the Kruskal-Wallis test (non-parametric) with the Dunn's multiple comparison test.

References

1. Jinek, M. et al. A programmable dual-RNA-guided DNA endonuclease in adaptive bacterial immunity. *Science* **337**, 816-821 (2012).
2. Bortesi, L. & Fischer, R. The CRISPR/Cas9 system for plant genome editing and beyond. *Biotechnology Advances* **33**, 41-52 (2015).
3. Lloyd, J.P., Seddon, A.E., Moghe, G.D., Simenc, M.C. & Shiu, S.H. Characteristics of Plant Essential Genes Allow for within-and between-Species Prediction of Lethal Mutant Phenotypes. *Plant Cell* **27**, 2133-2147 (2015).
4. Burgos-Rivera, B. & Dawe, R.K. An Arabidopsis Tissue-Specific RNAi Method for Studying Genes Essential to Mitosis. *Plos One* **7**, 7 (2012).
5. Tretter, E.M., Alvarez, J.P., Eshed, Y. & Bowman, J.L. Activity range of Arabidopsis small RNAs derived from different biogenesis pathways. *Plant Physiology* **147**, 58-62 (2008).
6. Mitsuda, N. et al. in Plant Transcription Factors: Methods and Protocols. (eds. L. Yuan & S.E. Perry) 87-105 (Humana Press, Totowa, NJ; 2011).
7. Fukaki, H., Nakao, Y., Okushima, Y., Theologis, A. & Tasaka, M. Tissue-specific expression of stabilized SOLITARY-ROOT/IAA14 alters lateral root development in Arabidopsis. *Plant Journal* **44**, 382-395 (2005).
8. Sieburth, L.E., Drews, G.N. & Meyerowitz, E.M. Non-autonomy of AGAMOUS function in flower development: use of a Cre/loxP method for mosaic analysis in Arabidopsis. *Development* **125**, 4303-4312 (1998).
9. Munoz-Nortes, T., Candela, H. & Micol, J.L. Suitability of two distinct approaches for the high-throughput study of the post-embryonic effects of embryo-lethal mutations in Arabidopsis. *Scientific Reports* **7**, 12 (2017).
10. Ablain, J., Durand, E.M., Yang, S., Zhou, Y. & Zon, L.I. A CRISPR/Cas9 Vector System for Tissue-Specific Gene Disruption in Zebrafish. *Developmental Cell* **32**, 756-764 (2015).
11. Port, F., Chen, H.M., Lee, T. & Bullock, S.L. Optimized CRISPR/Cas tools for efficient germline and somatic genome engineering in Drosophila. *Proceedings of the National Academy of Sciences of the United States of America* **111**, E2967-E2976 (2014).
12. Carroll, K.J. et al. A mouse model for adult cardiac-specific gene deletion with CRISPR/Cas9. *Proceedings of the National Academy of Sciences of the United States of America* **113**, 338-343 (2016).
13. Willemsen, V. et al. The NAC Domain Transcription Factors FEZ and SOMBRERO Control the Orientation of Cell Division Plane in Arabidopsis Root Stem Cells. *Developmental Cell* **15**, 913-922 (2008).
14. Fendrych, M. et al. Programmed Cell Death Controlled by ANAC033/SOMBRERO Determines Root Cap Organ Size in Arabidopsis. *Current Biology* **24**, 931-940 (2014).
15. Ingouff, M. et al. Live-cell analysis of DNA methylation during sexual reproduction in Arabidopsis reveals context and sex-specific dynamics controlled by noncanonical RdDM. *Genes & Development* **31**, 72-83 (2017).
16. Engler, C., Kandzia, R. & Marillonnet, S. A One Pot, One Step, Precision Cloning Method with High Throughput Capability. *PLoS One* **3**, 7 (2008).
17. Lampropoulos, A. et al. GreenGate - A Novel, Versatile, and Efficient Cloning System for Plant Transgenesis. *Plos One* **8**, 15 (2013).
18. Marzec, M. & Hensel, G. Targeted Base Editing Systems Are Available for Plants. *Trends Plant Sci* (2018).

19. Lowder, L.G. et al. A CRISPR/Cas9 Toolbox for Multiplexed Plant Genome Editing and Transcriptional Regulation. *Plant Physiology* **169**, 971-+ (2015).
20. Shimada, T.L., Shimada, T. & Hara-Nishimura, I. A rapid and non-destructive screenable marker, FAST, for identifying transformed seeds of Arabidopsis thaliana. *Plant J.* **61**, 519-528 (2010).
21. Cermak, T. et al. A Multipurpose Toolkit to Enable Advanced Genome Engineering in Plants. *Plant Cell* **29**, 1196-1217 (2017).
22. Brinkman, E.K., Chen, T., Amendola, M. & van Steensel, B. Easy quantitative assessment of genome editing by sequence trace decomposition. *Nucleic Acids Research* **42**, 8 (2014).
23. Nadeau, J.A. & Sack, F.D. Control of stomatal distribution on the Arabidopsis leaf surface. *Science* **296**, 1697-1700 (2002).
24. Ohashi-Ito, K. & Bergmann, D.C. Arabidopsis FAMA controls the final proliferation/differentiation switch during stomatal development. *Plant Cell* **18**, 2493-2505 (2006).
25. Qin, G.J. et al. Disruption of phytoene desaturase gene results in albino and dwarf phenotypes in Arabidopsis by impairing chlorophyll, carotenoid, and gibberellin biosynthesis. *Cell Research* **17**, 471-482 (2007).
26. Bergmann, D.C., Lukowitz, W. & Somerville, C.R. Stomatal development and pattern controlled by a MAPKK kinase. *Science* **304**, 1494-1497 (2004).
27. Lukowitz, W., Roeder, A., Parmenter, D. & Somerville, C. A MAPKK kinase gene regulates extra-embryonic cell fate in Arabidopsis. *Cell* **116**, 109-119 (2004).
28. De Rybel, B. et al. A Novel Aux/IAA28 Signaling Cascade Activates GATA23-Dependent Specification of Lateral Root Founder Cell Identity. *Current Biology* **20**, 1697-1706 (2010).
29. Okushima, Y., Fukaki, H., Onoda, M., Theologis, A. & Tasaka, M. ARF7 and ARF19 regulate lateral root formation via direct activation of LBD/ASL genes in Arabidopsis. *Plant Cell* **19**, 118-130 (2007).
30. Okushima, Y. et al. Functional genomic analysis of the AUXIN RESPONSE FACTOR gene family members in Arabidopsis thaliana: Unique and overlapping functions of ARF7 and ARF19. *Plant Cell* **17**, 444-463 (2005).
31. Meinke, D., Muralla, R., Sweeney, C. & Dickerman, A. Identifying essential genes in Arabidopsis thaliana. *Trends in Plant Science* **13**, 483-491 (2008).
32. Barton, K.A. et al. Epidermal Pavement Cells of Arabidopsis Have Chloroplasts. *Plant Physiology* **171**, 723-726 (2016).
33. Lawson, T. Guard cell photosynthesis and stomatal function. *New Phytologist* **181**, 13-34 (2009).
34. Negi, J. et al. Eukaryotic lipid metabolic pathway is essential for functional chloroplasts and CO2 and light responses in Arabidopsis guard cells. *Proceedings of the National Academy of Sciences of the United States of America* **115**, 9038-9043 (2018).
35. Musielak, T.J. & Bayer, M. YODA signalling in the early Arabidopsis embryo. *Biochemical Society Transactions* **42**, 408-412 (2014).
36. Smekalova, V. et al. Involvement of YODA and mitogen activated protein kinase 6 in Arabidopsis post-embryogenic root development through auxin up-regulation and cell division plane orientation. *New Phytol* (2014).
37. Kumpf, R.P. & Nowack, M.K. The root cap: a short story of life and death. *Journal of Experimental Botany* **66**, 5651-5662 (2015).
38. Lewsey, M.G. et al. Mobile small RNAs regulate genome-wide DNA methylation. *Proceedings of the National Academy of Sciences of the United States of America* **113**, E801-E810 (2016).
39. De Smet, I. et al. Bimodular auxin response controls organogenesis in Arabidopsis. *Proceedings of the National Academy of Sciences of the United States of America* **107**, 2705-2710 (2010).

40. Shemer, O., Landau, U., Candela, H., Zemach, A. & Williams, L.E. Competency for shoot regeneration from Arabidopsis root explants is regulated by DNA methylation. *Plant Science* **238**, 251-261 (2015).
41. Schurholz, A.K. et al. A Comprehensive Toolkit for Inducible, Cell Type-Specific Gene Expression in Arabidopsis. *Plant physiology* (2018).
42. von Wangenheim, D. et al. Rules and Self-Organizing Properties of Post-embryonic Plant Organ Cell Division Patterns. *Current Biology* **26**, 439-449 (2016).
43. Fu, J.L., Kanno, T., Liang, S.C., Matzke, A.J.M. & Matzke, M. GFP Loss-of-Function Mutations in Arabidopsis thaliana. *G3-Genes Genomes Genetics* **5**, 1849-1855 (2015).
44. Houbaert, A. et al. POLAR-guided signaling complex

assembly and localization drive asymmetric cell division. **Accepted on 26/09/2018** (2018).
45. Lennen, R.M. et al. Transient overexpression of DNA adenine methylase enables efficient and mobile genome engineering with reduced off-target effects. *Nucleic Acids Research* **44**, 14 (2016).
46. Pasin, F., Kulasekaran, S., Natale, P., Simon-Mateo, C. & Garcia, J.A. Rapid fluorescent reporter quantification by leaf disc analysis and its application in plant-virus studies. *Plant Methods* **10**, 11 (2014).
47. Karimi, M., De Meyer, B. & Hilson, P. Modular cloning in plant cells. *Trends in Plant Science* **10**, 103-105 (2005).
48. Xing, H.L. et al. A CRISPR/Cas9 toolkit for multiplex genome editing in plants. *Bmc Plant Biology* **14**, 12 (2014).
49. Clough, S.J. & Bent, A.F. Floral dip: a simplified method for *Agrobacterium*-mediated transformation of Arabidopsis thaliana. *Plant Journal* **16**, 735-743 (1998).
50. Schindelin, J. et al. Fiji: an open-source platform for biological-image analysis. *Nature Methods* **9**, 676-682 (2012).
51. Ursache, R., Andersen, T.G., Marhavy, P. & Geldner, N. A protocol for combining fluorescent proteins with histological stains for diverse cell wall components. *Plant Journal* **93**, 399-412 (2018).
52. Kurihara, D., Mizuta, Y., Sato, Y. & Higashiyama, T. ClearSee: a rapid optical clearing reagent for whole-plant fluorescence imaging. *Development* **142**, 4168-4179 (2015).
53. Sommer, C., Straehle, C., Kothe, U., Hamprecht, F.A. & Ieee ILASTIK: INTERACTIVE LEARNING AND SEGMENTATION TOOLKIT. *2011 8th Ieee International Symposium on Biomedical Imaging: from Nano to Macro*, 230-233 (2011).
54. Bargmann, B.O.R. & Birnbaum, K.D. Fluorescence Activated Cell Sorting of Plant Protoplasts. *JoVE*, e1673 (2010).

Acknowledgements

We thank Dominique Bergmann, Camila Lopez-Anido, Michael Raissig, and the members of the Programmed Cell Death and Plant Genome Editing teams at VIB for constructive discussions. We also thank Veronique Storme for assistance with statistical analysis. The GreenGate plasmid kit used for generation of plant transformation constructs was a gift from Jan Lohmann (Addgene kit # 1000000036). The coding sequence for mRuby3 was derived from pNCS-mRuby3, which was a gift from Michael Lin (Addgene plasmid # 74234). We thank Carina Braeckman (VIB-UGent Center for Plant Systems Biology) for the help with the *A. thaliana* floral dip transformation. We thank Nico Smet, Miguel Riobello y Barea, Thomas Farla, and Sandra Lefftz for greenhouse support. We thank Debbie Rombaut and Freya De Winter for the help with the preparation of root protoplasts. We thank Eugenia Russinova for a critical review of the manuscript. We gratefully acknowledge funding by the ERC StG PROCELLDEATH (Project 639234) to M.K.N., and by the FWO 1174119N to M.L.P.

Author contributions

W.D., R.A.B., M.K.N., and T.B.J. conceived and devised the study. M.K. adapted the GreenGate vectors and provided additional cloning support. W.D. constructed the vectors and performed the genotyping analysis. R.A.B., M.L.P., N.V. and J.J. performed the experiments, imaging and analysis. W.D., and R.A.B. performed statistical analysis. G.V.I. and R.A.B. performed the FACS experiments and analysis. W.D., T.B.J., R.A.B., M.K.N. and T.B. wrote the manuscript with contributions from all other authors.

Additional information

Supplementary information accompanies this paper at

Supplementary Table 1. Overview of plasmids

Supplementary Table 2. gRNA target sequences, with the PAM in bold

Supplementary Table 3. Primers used

Conflicts of interest

The authors declare no conflicts of interest.